Available online at www.sciencedirect.com
SCIENCE DIRECT®
Journal of Organometallic Chemistry 690 (2005) 2200–2208
Journal of Organometallic Chemistry
www.elsevier.com/locate/jorganchem

Effect of the organic fragment on the mesogenic properties of a series of organogold(I) isocyanide complexes. X-ray crystal structure of $[Au(C{\equiv}CC_5H_4N)(CNC_6H_4O(O)CC_6H_4OC_{10}H_{21})]$

Montserrat Ferrer [a,*], Mounia Mounir [a], Laura Rodríguez [a], Oriol Rossell [a], Silverio Coco [b], Pilar Gómez-Sal [c], Avelino Martín [c]

[a] *Departament de Química Inorgànica, Universitat de Barcelona, c/ Martí i Franquès 1-11, 08028 Barcelona, Spain*
[b] *Departamento de Química Inorgànica, Facultad de Ciencias, Universidad de Valladolid, 47005 Valladolid, Spain*
[c] *Departamento de Química Inorgánica, Campus Universitario-Edificio de Farmacia, Universidad de Alcalá, 28871 Alcalá de Henares, Spain*

Received 17 January 2005; revised 15 February 2005; accepted 16 February 2005

Abstract

Rod-like organogold(I) complexes $[AuR(CNC_6H_4O(O)CC_6H_4OC_{10}H_{21}\text{-}p)]$ were prepared and their liquid crystal behaviour was studied. Depending on the nature of R, the synthetic methodology was different. Thus, for R = substituted alkynyl ligands, the new compounds were prepared in two steps:(i) reaction of [AuCl(tht)] (tht = tetrahydrothiophene) with $R'C{\equiv}CH$($R' = C_5H_4N$, $C_6H_4C{\equiv}N$, $C_6H_4C{\equiv}CC_5H_4N$) in the presence of NaOAc to give insoluble $[Au(C{\equiv}CR')]_n$; (ii) reaction of the latter polymers with the isonitrile $CNC_6H_4O(O)CC_6H_4OC_{10}H_{21}\text{-}p$.For R = fluorinated aryls, the complexes were prepared by displacement of tht from the compounds [AuR(tht)] ($R = C_5F_4N$, $C_6F_4C_5H_4N$, C_6F_5) with isonitrile.In addition, an unexpected ionic derivative $[Au(C{\equiv}CC_5H_4NC_{10}H_{21})_2][Au(C{\equiv}CC_5H_4N)_2]$ was formed in the reaction between $[PPh_4][Au(C{\equiv}CC_5H_4N)_2]$ and $C_{10}H_{21}I$. All these compounds have been characterized by IR and NMR spectroscopy and mass spectrometry. The X-ray crystal structure of the compound with $R = C{\equiv}CC_5H_4N$ shows a linear molecule in which the gold atom is surrounded by the pyridine-containing acetylene and the isonitrile ligand, and no direct gold–gold interaction occurs. Six of the neutral compounds are liquid crystals and their optical, thermal and thermodynamic data were analyzed and compared in terms of molecular polarizability.

Keywords: Organogold compounds; Isocyanide; Liquid crystals; Alkynyl ligand; Fluoroaryl ligand

1. Introduction

In the course of our studies on supramolecular chemistry, we focused on a series of linear ditopic acetylide-based gold(I) compounds [1] because of their potential to construct supramolecular polygons such as triangles, squares and more complex structures by metal-directed self-assembly reactions [2,3]. On the other hand, a number of gold acetylide compounds have been shown to be excellent precursors for species showing liquid crystal behaviour because of the linear shape of the M—C≡C—R moiety and the lack of β-hydrogen atoms in the M—C≡C bond [4]. Looking at this second point, it is worth noting that linear gold complexes containing substituted acetylide groups may easily incorporate, through well established methods [5], ligands, such as isonitriles, that can give to the resulting species liquid crystalline properties. Less known for this purpose are the gold compounds containing fluorinated aryl rings [6], which interestingly, render more thermally stable

* Corresponding author. Tel.: +34 93 403 91 31; fax: +34 93 490 77 25.
E-mail address: montse.ferrer@qi.ub.es (M. Ferrer).

0022-328X/$ - see front matter © 2005 Elsevier B.V. All rights reserved.
doi:10.1016/j.jorganchem.2005.02.043

compounds. Although the understanding of the structure–property relationships of the gold-containing liquid crystals is reasonably good, much work still needs to be done. To this end, we undertook the synthesis of a series of new isonitrile gold complexes bearing acetylene or fluoroaryl ligands in order to study and compare the mesogenic behaviour of both groups of complexes.

2. Results and discussion

2.1. Synthesis and characterization

The isonitrile gold(I) complexes were prepared following different synthetic methods. [AuCl(CNC_6H_4-O(O)$CC_6H_4OC_{10}H_{21}$)] (**1**) was obtained by reacting [AuCl(tht)] with the isonitrile $CNC_6H_4O(O)CC_6H_4O$-$C_{10}H_{21}$-*p* in a CH_2Cl_2 solution at room temperature. Compounds **2b**, **3b** and **4b** were synthesized in good yields using the reactions outlined in Scheme 1, following a well-known strategy [5]. Firstly, the free acetylenes were reacted with [AuCl(tht)] (tht = tetrahydrothiophene) in the presence of NaOAc as base to give the insoluble $[Au(C{\equiv}CR')]_n$ derivatives (**2a**, **3a** and **4a**). In the next step, a suspension of the latter compounds in toluene was treated with the isonitrile $CNC_6H_4O(O)C$-$C_6H_4OC_{10}H_{21}$-*p* at room temperature to yield the soluble complexes **2b**, **3b** and **4b**.

Compound **5** was obtained by reacting $[PPh_4][Au(C{\equiv}CC_5H_4N)_2]$ with $C_{10}H_{21}I$ in a 1:10 molar ratio in CH_2Cl_2 at 40 °C for four days (Eq. (1)). The product was precipitated from the solution as grey solid in reasonably good yields. The formation of **5** can be rationalized on the basis of a ligand redistribution process of the intermediate $[Au(C{\equiv}CC_5H_4N)(C{\equiv}CC_5H_4NC_{10}H_{21})]$.

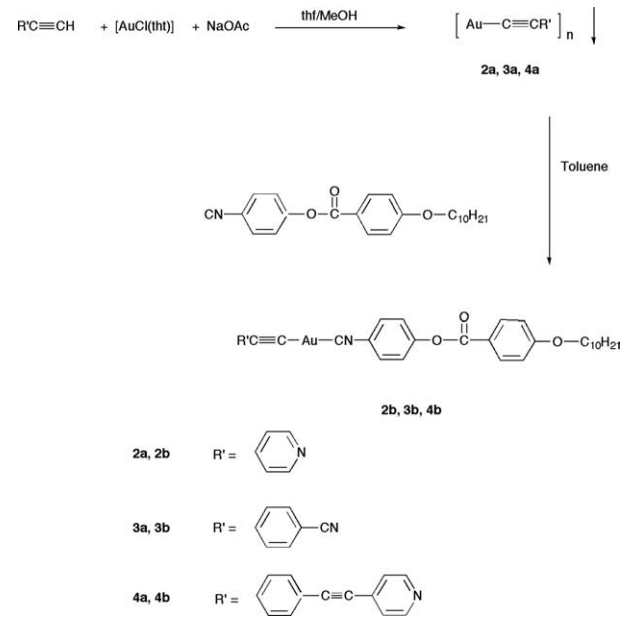

Scheme 1.

compounds in which the triple bond is coordinated to gold.

All the other complexes have been characterized by C, H, N analyses, IR and NMR spectroscopy and mass spectrometry. In addition, the molecular structure of **2b** has been solved by X-ray diffraction analysis. The IR spectra of **2b**–**4b** show one band for the C≡CAu stretch, slightly shifted to higher energy (ca. 5 cm^{-1}) in relation to the starting polymers. In addition, **4b** displays another C≡C absorption at 2214 cm^{-1} due to the alkynyl unit unbonded to the metal. The isonitrile derivatives present one C≡N band that appears in the 2215–2225 cm^{-1} region at about 100 cm^{-1} higher wavenumbers than for the free isonitrile. The increase in the

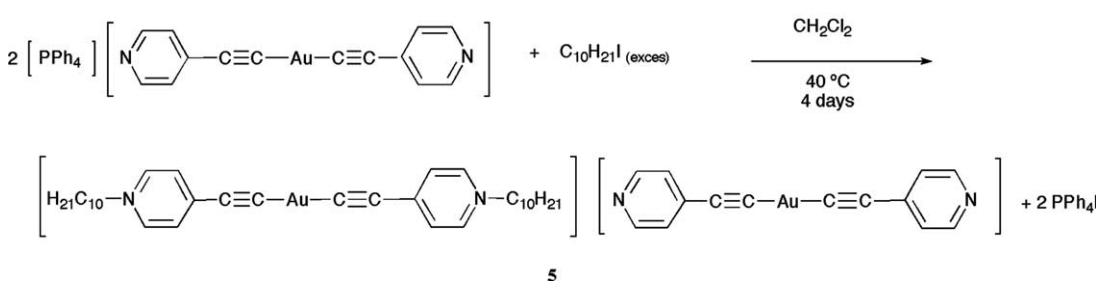

(1)

6b–**8b** were synthesized by displacement of tetrahydrotiophene from [AuR(tht)] (R = C_5F_4N, $C_6F_4C_5H_4N$ and C_6F_5) by the isonitrile: (Scheme 2).

The three $[Au(C{\equiv}CR')]_n$ (**2a**–**4a**) are pale yellow solids that are insoluble in common non-coordinating solvents. Elemental analyses support the stoichiometry. The IR spectra show only one C≡C absorption in the range 2116–2126 cm^{-1}, as expected for polymeric CN stretching frequency of coordinated isocyanide is attributed to the σ donation of the antibonding carbon lone pair to gold upon complexation [7]. FAB(+) mass spectra of **1**, **2b**–**4b** and **6b**–**8b** contain the molecular peaks, corresponding in most of the cases to $[M+H^+]$ (Section 3).

The ^1H NMR spectra of compounds **1**, **2b**–**4b**, **6b**–**8b** show four distorted doublets in the range 8.12–6.99 ppm

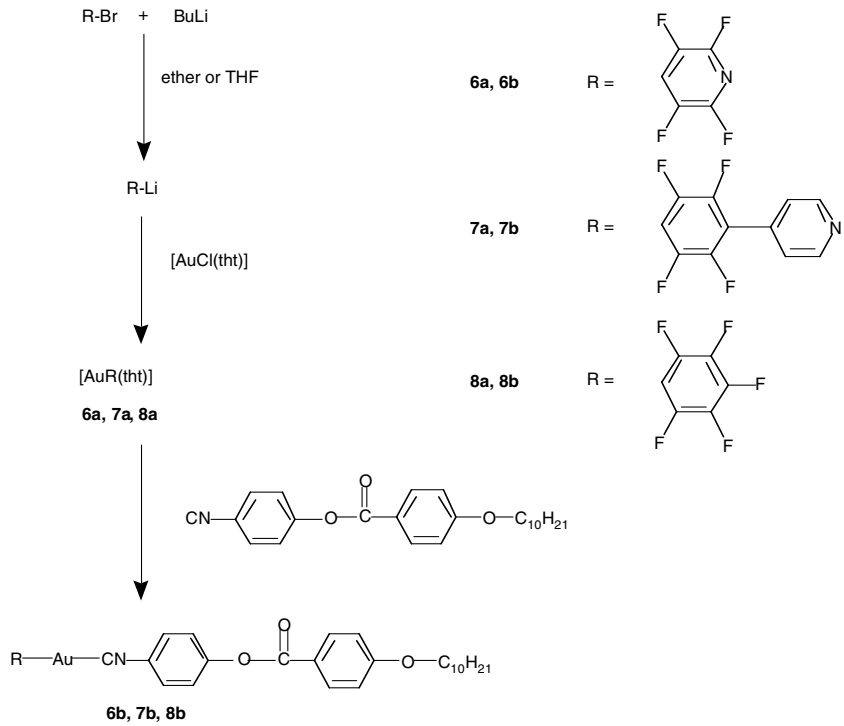

Scheme 2.

with apparent coupling constants of 8.7–8.9 Hz that correspond to the aromatic hydrogens of the isonitrile rings. In addition, the first methylene group of the alkoxy chain of the isonitrile group is observed as a triplet centred at 4.05 ppm in all cases and the remaining chain hydrogens appear in the range 1.85–0.85 ppm.

The hydrogens of the pyridine groups give rise to pairs of doublets (AA′XX′ spin system) at 8.48 ($H_{\alpha\text{-py}}$) and 7.31 ppm ($H_{\beta\text{-py}}$) (**2b**), 8.59 ($H_{\alpha\text{-py}}$) and 7.53 ppm ($H_{\beta\text{-py}}$) for compound **4b** and 8.71 ppm ($H_{\alpha\text{-py}}$) and 7.40 ppm ($H_{\beta\text{-py}}$) for **7b**. Apparent coupling constants are 6.0, 4.4 and 5.5 Hz, respectively. Compounds **3b** and **4b** show a singlet (**3b**) or a multiplet (**4b**) for the four hydrogens of the aromatic rings linked to the triple bond.

The ^{1}H NMR spectrum of compound **5** shows four multiplets between 8.77 and 7.11 ppm, with the protons of the pyridine group linked to the alkyl chain (8.77 and 7.80 ppm) downfield in comparison with the respective pyridine protons of the anion (8.35 and 7.11 ppm). Alkyl chain hydrogens show a pattern similar to that observed in compounds **1**, **2b**–**4b**, **6b**–**8b**.

The ^{19}F NMR of compounds **6b** and **7b** are very similar. In both cases, there are two types of signals corresponding to the two different types of fluorine atoms. For **6b**, the signals correspond to an AA′XX′ spin system and appear at −98.5 and −124.0 ppm, and they are assigned to F_{ortho} and F_{meta} to gold, respectively. For **7b**, the signals correspond to a more complex spin system, because the F_{meta} to gold present an additional coupling with the aromatic hydrogens of the pyridine ring, and appear at −118.9 (F_{ortho}) and −147.1 ppm (F_{meta}). Compound **8b** presents three different types of fluorine atoms whose chemical shifts are: −118.5, −159.9 and −164.9 ppm and were assigned to F_{ortho}, F_{para} and F_{meta}, respectively.

2.2. Crystal structure of *2b*

Crystals for X-ray analysis were grown by ether vapour diffusion in a CH_2Cl_2 solution of **2b**. Unfortunately, after numerous trials only bad quality crystals could be obtained, but the interest of the structural disposition of the molecules encouraged us to perform the study. The structure of **2b** is shown in Fig. 1, together with the atomic numbering scheme; the most significant bond distances and angles are listed in Table 1.

The molecule has, as expected, an extended close linear structure where the C(7)AuC(8), C(7)C(6)C(3) and C(8)N(2)C(9) angles show a slight deviation from the ideal angle of 180°. In the crystal (Fig. 2), the molecules are packed as a bimolecular assembly with an antiparallel alignment of the two monomers. A close analysis reveals that no direct gold–gold interaction exists, in contrast with some reports in the literature [8]. Thus, the shortest intermolecular gold–gold distance is 6.835 Å, which is out of the range for considering a bonding interaction (ca. 2.75–3.40 Å).

If the standard deviations are taken into account, the structural parameters of **2b** are in the range found for other similar compounds [1,9], but unfortunately the poor quality of the resolution precludes a detailed comparison.

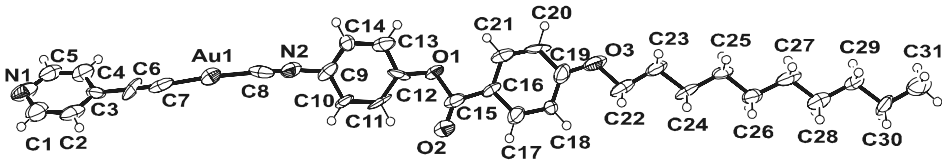

Fig. 1. ORTEP drawing of the molecular structure and numbering scheme of compound **2b**.

Table 1
Selected interatomic distances (Å) and bond angles (°) of **2b**

C(6)–C(7)	1.26(4)
C(7)–Au(1)	1.97(3)
C(8)–N(2)	1.17(3)
C(8)–Au(1)	1.99(3)
C(7)–C(6)–C(3)	177(3)
C(6)–C(7)–Au(1)	170(2)
N(2)–C(8)–Au(1)	175(2)
C(8)–N(2)–C(9)	173(2)
C(7)–Au(1)C(8)	172.8(9)

2.3. Mesogenic behaviour

The thermal behaviour of the complexes **1**, **2b**–**4b**, **5** and **6b**–**8b** (seven neutral complexes and an ionic derivative) was studied; six of them are liquid crystals. Their optical, thermal and thermodynamic data are collected in Table 2.

The free isonitrile displays smectic A and nematic mesophases in the range 68–84 °C [10]. Complexes **1**, **2b**, **3b**, **6b**, **7b** and **8b** derivatives display a SmA mesophase, which has been identified in optical microscopy by their typical oily streaks and homeotropic textures giving focal-conic texture at temperatures close to the clearing point (Fig. 3), and a fan-shaped texture on cooling from the isotropic phase (Fig. 4) [11–13]. Compound **1** shows, in addition to SmA, a second mesophase at lower temperatures. This mesophase displays a broken fan-shaped texture formed on cooling the fan-shaped area of the SmA phase, and regions with a schlieren mosaic texture formed on cooling the homeotropic regions of the SmA phase (Fig. 5). These observations are consistent with a smectic F mesophase [11–13]. In contrast, complex **4b** melts directly to an isotropic liquid with extensive decomposition, and the ionic derivative **5** decomposes at 219 °C without melting, thus they are not liquid crystals. For this reason, the data for both compounds **4b** and **5** are referred to the first DSC cycle.

Some of the complexes show crystal–crystal transitions before the melting temperature, and most of them undergo significant decomposition at the clearing temperature possibly due to the high transition temperatures. In addition, it is important to note that the alkynyl derivatives show the lowest thermal stability of the complexes described in this work. Most likely this behaviour is due to the high thermal lability of Au–alkynyl bond. However, it is remarkable that our alkynyl

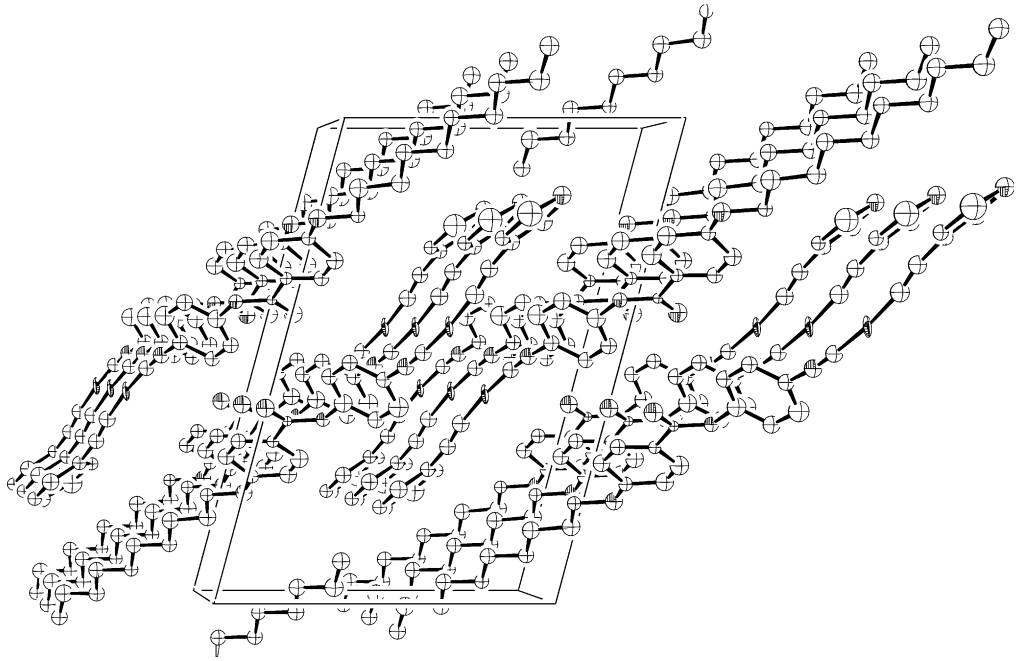

Fig. 2. View of the unit cell of **2b**, normal to the (100) plane.

Table 2
Optical, thermal and thermodynamic data of complexes $[AuR(CNC_6H_4O(O)CC_6H_4OC_{10}H_{21})]$ and $[Au(C{\equiv}CC_5H_4NC_{10}H_{21})_2]$-$[Au(C{\equiv}CC_5H_4N)_2]$

Compound	Transition[a]	Temperature[b] (°C)	ΔH[b] (KJ/mol)
1	C–SmF	132.2	18.3
	SmF–SmA	152.3	2.1
	SmA–I (dec)	270[c]	
2b	C–C′	113.2[d]	1.9
	C′–SmA	144.2[d]	25.2
	SmA–I (dec)	180.0[c,d]	[e]
3b	C_X–C_Y	55.9[d]	2.2[f]
	C_Y–SmA + C_W	103.2[d]	24.4
	C_W + SmA–C_W	120.5[d]	−6.5
	C_W–SmA	149.5[d]	19.9
	SmA–C_W	131.7	−14.5
	C_W–C_Z	59.0	−3.9[f]
	C_Z–SmA + C_M	58.0	4.0[f]
	SmA + C_M–C_W	105.5	−3.3
	C_W–SmA	146.9	18.6
	SmA–I (dec)	178.0[c]	
4b	C–I (dec)	175.0[c,d]	[e]
5	C–dec	219.0[c,d]	[e]
6b	C–SmA	94.7	49.7
	SmA–I	101.2	1.4
7b	C–C′	73.9	0.7
	C′–SmA	87.4	18.7[f]
	SmA–I (dec)	215.0[c]	[e]
8b	C–C′	88.8	1.8
	C′–SmA	126.9	24.6
	SmA–I	167.5	3.0

[a] C, crystal; C_X, C_Y, C_Z, C_W, C_M, uncharacterized crystalline phases; Sm, smectic; I, isotropic liquid.
[b] Data referred to the second DSC cycle starting from the crystal. Temperature data as peak onset.
[c] Microscopic data.
[d] Data referred to the first DSC cycle starting from the crystal obtained by cooling the SmA mesophase.
[e] Decomposition precludes measurement.
[f] Combined enthalpies. dec, decomposition.

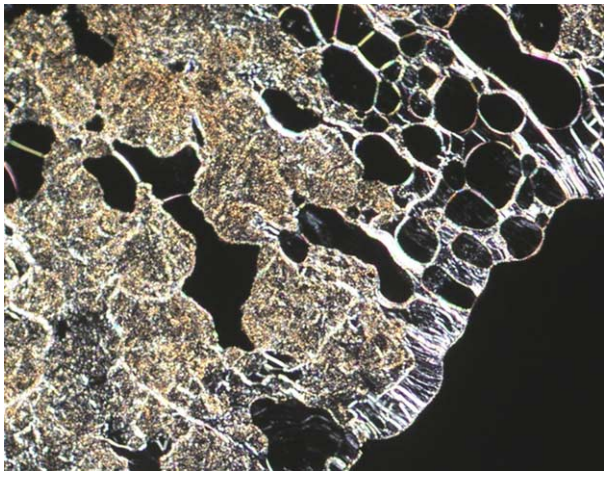

Fig. 3. Polarized optical microscopic textures (100×) observed for **2b** obtained on heating from the solid at 155 °C. The picture shows oily streaks and homeotropic zones.

Fig. 4. Polarized optical microscopic fan-shaped texture (100×) observed for **6b** obtained on cooling from the isotropic liquid at 95 °C.

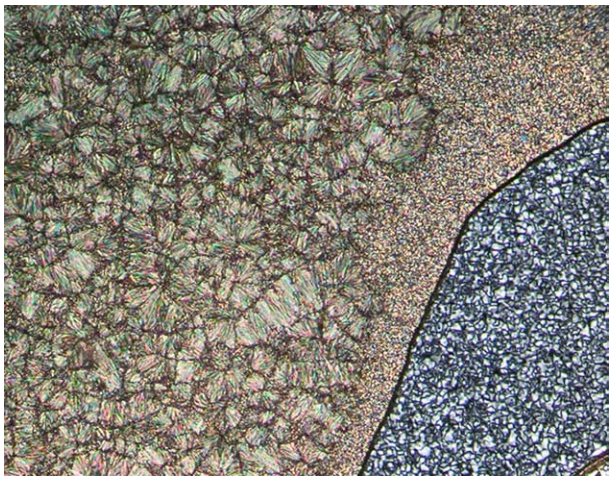

Fig. 5. Polarized optical microscopic texture (100×) for **1** at 160 °C. The picture shows the broken fan-shaped texture of the SmF phase formed on cooling from the fan-shaped focal-conic area of the SmA phase, and a region with schlieren mosaic texture of the SmF phase formed on cooling the homeotropic region of the SmA phase.

gold isocyanide complexes show a slightly higher thermal stability than that of analogous mesomorphic gold alkynyl isocyanide complexes reported, which decompose at ca. 160 °C [4b,10].

The mesogenic derivative **3b** appears in several solid polymorphic forms with different melting points, and exhibits the so-called double melting behaviour via the SmA mesophase (Fig. 6) [14].

The variation in the melting temperatures of gold(I) complexes studied is quite regular, decreasing in the order: **5** > **4b** > **3b** > **2b** > **1** > **8b** > **6b** > **7b**.

Metal-containing liquid crystals can present intermolecular metal–metal interactions, and it has been suggested that such interactions are very important for the formation and stabilization of mesophases in these systems [10,15]. However, X-ray analysis has revealed

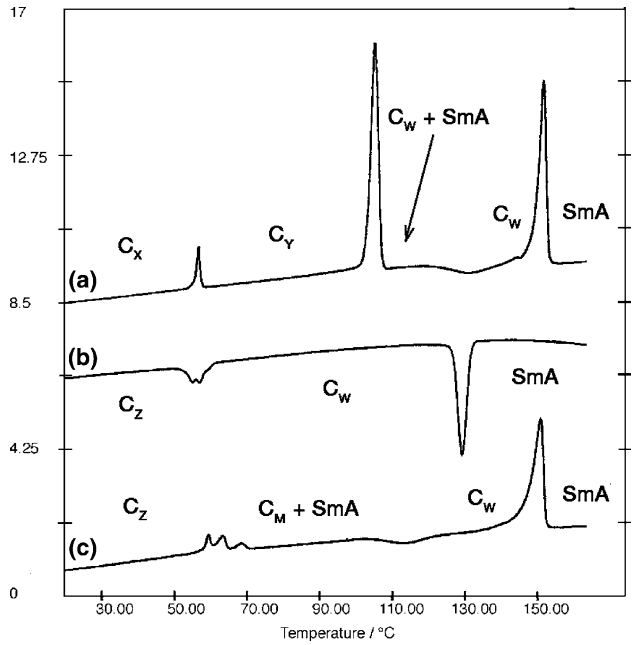

Fig. 6. DSC scans of **3b**. (a) First heating, (b) first cooling, (c) second heating.

that no gold–gold interactions are present in **2b**. Thus, it is obvious that the rather strong intermolecular interactions operating in **2b** are not due to metal–metal interactions. The same result was found for other mesogenic alkynylgold complexes [10].

In order to understand the thermal behaviour of the compounds studied here, they can be considered as formal derivatives of **1** by replacing the Cl ligand for an alkynyl group (compounds **2b**, **3b**, **4b**) or a perfluoroaryl ligand (derivatives **6b**, **7b**, **8b**). The introduction of alkynyl groups leads to higher values for the molecular polarizability as an alkynyl group is more polarizable than Cl, increasing intermolecular interactions and leading to higher melting temperatures [16]. In addition, the variation in the size of the molecule on going from Cl to alkynyl groups produces an increase in the total length of the molecule, whereas the molecular breadth (considered as a cylinder) increases slightly, since the latter is essentially determined by the bulkier benzoatephenylisocyanide ligand. Thus, the intermolecular interactions in the alkynyl derivatives should be stronger than in the chloro complex, leading to higher transition temperatures, as observed.

Analogously, **3b** and **4b** can be considered as formal derivatives of **2b** by replacing the pyridine group with a C_6H_4CN moiety (**3b**) and with a $C_6H_4C{\equiv}CC_5H_4N$ group (**4b**). The introduction of a C_6H_4CN substituent leads to higher values for the molecular polarizability as C_6H_4CN is more polarizable than the pyridine group [16], increasing intermolecular interactions and leading to higher transition temperatures. Thus, the melting temperature of **3b** should be higher than that of **2b**, as observed. Similarly, the polarizability of the $C_6H_4C{\equiv}CC_5H_4N$ group is clearly higher than that of C_5H_4N and C_6H_4CN groups, and as a consequence the melting temperatures should vary in the order **4b** > **3b** > **2b**, as experimentally found.

Comparing now the thermal properties of the chloro compound (**1**) with those of perfluoroaryl derivatives (**6b**, **7b**, **8b**) (Table 2), it can be seen that the perhalophenyl groups produce lower transition temperatures, shorter mesogenic ranges, and an enhancement of SmA phases, according to the expected lower lateral intermolecular interactions as a consequence of their greater molecular width. In keeping with the variation of the polarizabilities and the previous discussion, the melting temperatures should decrease in the order **7b** > **8b** > **6b**; however, the variation experimentally found is **8b** > **6b** > **7b**. It is known that in 4-perfluorophenylpyridines the perfluorophenyl ring is significantly twisted with respect to the plane of the pyridine ring [17,18]. This non-planar structure must necessarily reduce the intermolecular interactions leading to lower melting temperatures.

Compound **5** is very different from the rest, because its structure contains two alkyl chains and in addition it is an ionic species. An increase of the number of the alkyl chains can cause an increase in the degree of disorder associated with the chains, producing lower transition temperatures. However, the molecular arrangement of an ionic complex made up of anisotropic organometallic ions is due to both electrostatic and van der Waals interactions between the fragments that constitute the complex [19]. These factors produce an increase in the intermolecular interactions leading to higher transition temperatures. Thus, it is not surprising that the ionic compound **5** shows the highest melting temperature.

3. Experimental

3.1. General

All manipulations were performed under prepurified N_2 using standard Schlenk techniques. All solvents were distilled from appropriate drying agents. Infrared spectra were recorded on an FT-IR 520 Nicolet spectrophotometer. ^{1}H NMR (δ(TMS) = 0.0 ppm) spectra were obtained on a Bruker DXR 250, Varian Gemini 200, Varian Unity 300 and Varian Mercury 400 spectrometers. ^{19}F NMR ($\delta(CFCl_3)$ = 0.0 ppm) spectra were obtained on a Varian Unity 300 and Varian Mercury 400 spectrometers. Elemental analyses of C, H and N were carried out at the Institut de Bio-Orgànica in Barcelona. FAB mass spectra were recorded on a Fisons VG Quattro spectrometer. Microscopy studies were carried out using a Leitz microscope provided with a hot stage and polarizers at a heating rate of approx. 10 °C min^{-1}.

For differential scanning calorimetry (DSC) a Perkin–Elmer DSC7 instrument was used, which was calibrated with water and indium; the scanning rate was 10 °C min^{-1}, the samples were sealed in aluminium capsules in the air, and the holder atmosphere was dry nitrogen. Literature methods were used to prepare [$CNC_6H_4O(O)CC_6H_4OC_{10}H_{21}$-*p*] [10], [AuCl(tht)] [20], 4-ethynylpyridyne [21], 4-ethynylbenzonitrile [22], (4-ethynylphenyl)(4-pyridyl)acetylene [23], 4-(4-bromotetrafluorophenyl)pyridine [18], [$Au(C_6F_5)$(tht)] (**8a**) [20] and [PPh_4][$Au(C{\equiv}CC_5H_4N)_2$] [1].

3.2. Synthesis and characterization data

3.2.1. Synthesis of [$AuCl(CNC_6H_4O(O)CC_6H_4OC_{10}H_{21})$] (**1**)

Solid $CNC_6H_4O(O)CC_6H_4OC_{10}H_{21}$ (120 mg, 0.32 mmol) was added to a dichloromethane (15 ml) solution of [AuCl(tht)] (100 mg, 0.32 mmol). After 15 min of stirring a white solid was obtained. The addition of hexane favours the precipitation of compound **1**. During all the manipulations, the solution was protected from the light in order to avoid decomposition. Yield: 90%. IR (KBr, cm^{-1}), 2919 s, 2851 s, ν(C–H); 2235 s, ν(C≡N); 1724 s, ν(C≡O). ^1H NMR (298 K, $CDCl_3$): 8.10 (d, *J*(H–H) = 9.0 Hz, 2H, (O)C–C_6H_4–O), 7.60 (d, *J*(H–H) = 9.1 Hz, 2H, CN–C_6H_4–O), 7.38 (d, *J*(H–H) = 9.1 Hz, 2H, CN–C_6H_4–O), 6.97 (d, *J*(H–H) = 9.0 Hz, 2H, (O)C–C_6H_4–O), 4.05 (t, 2H, *J*(H–H) = 6.6 Hz, 2H, CH_2–O–C_6H_4), 1.84–1.27 (m, 16H, C_8H_{16}), 0.89 (t, *J*(H–H) = 6.3 Hz, 3H, CH_3). FAB(+) *m/z*: 1187.4 (2M − Cl, calc.: 1187.4), 1030.6 (2M − Cl − $OC_{10}H_{21}$, calc.: 1030.4). Anal. Calc. for $C_{24}H_{29}AuClNO_3$: C, 47.11; H, 4.78; N, 2.29. Found: C, 47.15; H, 4.78; N, 2.34%.

3.2.2. Synthesis of [$Au(C{\equiv}CC_5H_4N)]_n$ (**2a**)

Solids [AuCl(tht)] (155 mg, 0.49 mmol) and NaOAc (199 mg, 2.45 mmol) were added to a thf/MeOH 1:1 (14 ml) solution of 4-ethynylpyridine (50 mg, 0.49 mmol) at room temperature. After 30 min of stirring, a pale yellow solid was obtained, which was washed with methanol and thf. During all the manipulations, the solution was protected from the light in order to avoid gold deposition. Yield: 71%. IR (KBr, cm^{-1}), 2126 s, ν(C≡C). Anal. Calc. for C_7H_4AuN: C, 28.11; H, 1.35; N, 4.68. Found: C, 28.14; H, 1.32; N, 4.70%.

3.2.3. Syntheses of [$Au(C{\equiv}CC_6H_4CN)]_n$ (3a) and [$Au(C{\equiv}CC_6H_4C{\equiv}CC_5H_4N)]_n$ (**4a**)

Details of synthesis of **2a** also applied to **3a** and **4a**.

3a: Yield: 65%. IR (KBr, cm^{-1}): 2228 m, ν(C≡N), 2116 w, ν(C≡C). Anal. Calc. for C_9H_4AuN: C, 33.46; H, 1.25; N, 4.34. Found: C, 33.47; H, 1.28; N, 4.35%.

4a: Yield 60%. IR (KBr, cm^{-1}): 2214 m, ν(pyC≡C); 2122 w, ν(C≡CAu). Anal. Calc. for $C_{15}H_8AuN$: C, 45.13; H, 2.02; N, 3.51. Found: C, 45.05; H, 2.03; N, 3.49%.

3.2.4. Synthesis of [$Au(C{\equiv}CC_5H_4N)(CNC_6H_4O(O)CC_6H_4OC_{10}H_{21})$] (**2b**)

Solid $CNC_6H_4O(O)CC_6H_4OC_{10}H_{21}$ (51 mg, 0.13 mmol) was added to a toluene (7 ml) suspension of [$Au(C{\equiv}CC_5H_4N)]_n$ (40 mg, 0.13 mmol). After 15 min of stirring, the resulting suspension was concentrated to dryness under vacuum and washed with hexane. The solid residue was dissolved in dichloromethane (2 ml) and the addition of diethylether caused the precipitation of compound **2b** as a white solid. Yield: 60%. IR (KBr, cm^{-1}), 2920 s, 2851 m, ν(C–H); 2221 m, ν(C≡N); 2130 w, ν(C≡C); 1729 s, ν(C≡O). ^1H NMR (298 K, $CDCl_3$): 8.48 (d, *J*(H–H) = 6.0 Hz, 2H, $H_{\alpha\text{-py}}$), 8.11 (d, *J*(H–H) = 8.9 Hz, 2H, (O)C–C_6H_4–O), 7.61 (d, *J*(H–H) = 9.0 Hz, 2H, CN–C_6H_4–O), 7.38 (d, *J*(H–H) = 8.9 Hz, 2H, (O)C–C_6H_4–O), 7.31 (d, *J*(H–H) = 6.0 Hz, 2H, $H_{\beta\text{-py}}$), 6.98 (d, *J*(H–H) = 9.0 Hz, 2H, CN–C_6H_4–O), 4.05 (t, *J*(H–H) = 6.6 Hz, 2H, CH_2–O–C_6H_4), 1.85–1.22 (m, 16H, C_8H_{16}), 0.88 (t, *J*(H–H) = 5.8 Hz, 3H, CH_3). FAB(+) *m/z*: 679.3 (M + H^+, calc.: 679.0). Anal. Calc. for $C_{31}H_{33}AuN_2O_3$: C, 54.87; H, 4.90; N, 4.13. Found: C, 54.85; H, 4.89; N, 4.16%.

3.2.5. Syntheses of [$Au(C{\equiv}CC_6H_4CN)(CNC_6H_4O(O)CC_6H_4OC_{10}H_{21})$] (**3b**) and [$Au(C{\equiv}CC_6H_4C{\equiv}C{-}C_5H_4N)(CNC_6H_4O(O)CC_6H_4OC_{10}H_{21})$] (**4b**)

Details of the synthesis of **2b** also applied to **3b** and **4b**.

3b: Yield: 65%. IR (KBr, cm^{-1}): 2920 s, 2853 m, ν(C–H), 2219 s, br, ν(C≡N—C_6H_4O(O)C) + ν(N≡C—C_6H_4—C≡C), 2122 w, ν(C≡C); 1737 s, ν(C≡O). ^1H NMR (298 K, $CDCl_3$): 8.11 (d, *J*(H–H) = 8.9 Hz, 2H, CO–C_6H_4–O), 7.61 (d, *J*(H–H) = 8.0 Hz, 2H, CN–C_6H_4–O), 7.52 (s, 4H, C≡CC_6H_4CN), 7.38 (d, *J*(H–H) = 8.0 Hz, 2H, CN–C_6H_4–O), 6.98 (d, *J*(H–H) = 8.9 Hz, 2H, (O)C–C_6H_4–O), 4.05 (t, 2H, *J*(H–H) = 6.5 Hz, 2H, CH_2–O–C_6H_4), 1.85–1.28 (m, 16H, C_8H_{16}), 0.89 (t, *J*(H–H) = 6.3 Hz, 3H, CH_3). FAB(+) *m/z*: 703.3 (M + H^+, calc.: 703.0). Anal. Calc. for $C_{33}H_{33}AuN_2O_3$: C, 56.41; H, 4.73; N, 3.99. Found: C, 56.39; H, 4.72; N, 3.97%.

4b: Yield: 30%. IR (KBr, cm^{-1}): 2921 s, 2850 m, ν(C–H), 2220 w, br, ν(C≡N) + ν(pyC≡C), 2124 w, ν(C≡CAu), 1735 s, ν(C≡O). ^1H NMR (298 K, $CDCl_3$): 8.59 (d, *J*(H–H) = 4.4 Hz, 2H, $H_{\alpha\text{-py}}$), 8.11 (d, *J*(H–H) = 8.1 Hz, 2H, (O)C–C_6H_4–O), 7.61 (d, *J*(H–H) = 7.7 Hz, 2H, CN–C_6H_4–O), 7.57–7.53 (m, 4H, C≡CC_6H_4C≡C), 7.48 (d, *J*(H–H) = 7.7 Hz, 2H, CN–C_6H_4–O), 7.37 (m, 2H, $H_{\beta\text{-py}}$), 6.98 (d, *J*(H–H) = 8.1 Hz, 2H, (O)C–C_6H_4–O), 4.05 (t, 2H, *J*(H–H) = 6.3 Hz, 2H, CH_2–O–C_6H_4), 1.85–1.28 (m, 16H, C_8H_{16}), 0.88 (t, *J*(H–H) = 6.0 Hz, 3H, CH_3). FAB(+) *m/z*: 779.3 (M + H^+, calc.: 779.0). Anal. Calc. for

$C_{39}H_{37}AuN_2O_3$: C, 60.16; H, 4.79; N, 3.60. Found: C, 60.12; H, 4.77; N, 3.61%.

3.2.6. Synthesis of $[Au(C{\equiv}CC_5H_4NC_{10}H_{21})_2]$-$[Au(CCC_5H_4N)_2]$ (5)

$C_{10}H_{21}I$ (0.3 ml, 1.40 mmol) was added dropwise to a dichloromethane (25 ml) solution of $[PPh_4][Au(C{\equiv}C$-$C_5H_4N)_2]$ (100 mg, 0.14 mmol). After the resulting mixture was heated for four days at 40 °C, a grey solid was obtained in 40% yield. IR (KBr, cm^{-1}), 2922 s, 2853 m, ν(C–H); 2109 s, ν(C≡Cpy), 2088 m ν(C≡Cpy$C_{10}H_{21}$). ^{1}H NMR (298 K, dmso-d_6): 8.77 (m, 2H, $H_{\alpha\text{-py(cation)}}$), 8.35 (m, 2H, $H_{\alpha\text{-py(anion)}}$), 7.80 (m, 2H, $H_{\beta\text{-py(cation)}}$), 7.11 (m, 2H, $H_{\beta\text{-py(anion)}}$), 4.37 (m, 2H, CH_2–C_9H_{19}), 1.82–1.21 (m, 16H, C_8H_{16}), 0.82 (t, J(H–H) = 6.1 Hz, 3H, CH_3). FAB(+) m/z: 683.3 (M^+, calc.: 683.0), 543.2 ($M^+ - C_{10}H_{21} + H^+$, calc.: 543.0), 440.2 (M^+ – C≡Cpy$C_{10}H_{21}$, calc.: 440.0). FAB(−) m/z: 401.4 (M^-, calc.: 401.0). Anal. Calc. for $C_{48}H_{58}Au_2N_4$: C, 53.14; H, 5.39; N, 5.16. Found: C, 53.20; H, 5.39; N, 5.21%.

3.2.7. Synthesis of $[Au(C_5F_4N)(tht)]$ (6a)

n-BuLi (1.6 M in hexane) (3 ml, 0.31 mmol) was slowly added to a stirred diethyl ether solution (20 ml) of 4-bromotetrafluoropyridine (0.037 ml, 0.31 mmol) at −78 °C. After 1 h, the flask was shielded from light with aluminium foil, 100 mg (0.31 mmol) of [AuCl(tht)] were added and the mixture was stirred under a nitrogen atmosphere for 1 h while the temperature was maintained at −78 °C. After the mixture was allowed to warm to 15 °C, the precipitated LiCl was filtered off. The filtered solution was evaporated to 5 ml and the addition of hexane caused the precipitation of compound **6a**. Yield: 37%. IR (KBr, cm^{-1}): 1625 m, 1446 s, 1203 m, 921 m, (C_5F_4N). Anal. Calc. for $C_9H_8AuF_4NS$: C, 24.84; H, 1.85; N, 3.22; S, 7.37. Found: C, 24.73; H, 1.83; N, 3.18; S, 7.41%.

3.2.8. Synthesis of $[Au(C_6F_4C_5H_4N)(tht)]$ (7a)

Details of the synthesis of **6a** also applied to **7a**. Yield: 40%. IR (KBr, cm^{-1}): 1443 m, 946 m, (C_6F_4). Anal. Calc. for $C_{15}H_{12}AuF_4NS$: C, 35.24; H, 2.36; N, 2.74; S, 6.27. Found: C, 35.90; H, 2.38; N, 2.66; S, 6.55%.

3.2.9. Synthesis of $[Au(C_5F_4N)(CNC_6H_4O(O)$-$CC_6H_4OC_{10}H_{21})]$ (6b)

Solid $CNC_6H_4O(O)CC_6H_4OC_{10}H_{21}$ (26 mg, 0.07 mmol) was added to a dichloromethane (10 ml) solution of $[Au(C_5F_4N)(tht)]$ (**6a**) (30 mg, 0.07 mmol). After 45 min of stirring, the mixture was filtered to separate possible colloidal gold. The filtered solution was evaporated to 5 ml under vacuum. Addition of hexane (5 ml) caused the precipitation of a white solid which was filtered off to give **6b**. Yield: 40%. IR (KBr, cm^{-1}): 2221 s, ν(C≡N), 1730 s ν(C≡O), 1629 m, 1448 s, 1206 m, 923 s, (C_5F_4N). ^{1}H NMR (298 K, $CDCl_3$): 8.12 (d, J(H–H) = 8.9 Hz, 2H, (O)C–C_6H_4–O), 7.65 (d, J(H–H) = 8.8 Hz, 2H, CN–C_6H_4–O), 7.42 (d, J(H–H) = 8.9 Hz, 2H, (O)C–C_6H_4–O), 6.99 (d, J(H–H) = 9.0 Hz, 2H, CN–C_6H_4–O), 4.05 (t, J(H–H) = 6.7 Hz, 2H, –CH_2–O–C_6H_4), 1.83–1.28 (m, 16H, C_8H_{16}), 0.88 (t, J(H–H) = 6.8 Hz, 3H, CH_3). ^{19}F NMR (298 K, $CDCl_3$, coaxial tube of CF_3COOH in D_2O): −98.5 (m, 2F, F_o), −124.0 (m, 2F, F_m). FAB (+) m/z: 727.0 ($M + H^+$, calc.: 727.5). Anal. Calc. for $C_{29}H_{29}AuF_4N_2O_3$: C, 47.95; H, 4.02; N, 3.86. Found: C, 47.23; H, 4.04; N, 3.83%.

3.2.10. Syntheses of $[Au(C_6F_4C_5H_4N)(CNC_6H_4O(O)$-$CC_6H_4OC_{10}H_{21})]$ (7b) and $[Au(C_6F_5)(CNC_6H_4O(O)$-$CC_6H_4OC_{10}H_{21})]$ (8b)

Details of the synthesis of **6b** also applied to **7b** and **8b**.

7b: Yield: 40%. IR (KBr, cm^{-1}): 2216 s, ν(C≡N), 1730 s, ν(C≡O), 1448 m, 947 m, 824, (C_6F_4). ^{1}H NMR (298 K, $CDCl_3$): 8.71 (d, J(H–H) = 5.5 Hz, 2H, $H_{\alpha\text{-py}}$) 8.12 (m, 2H, (O)C–C_6H_4–O), 7.63 (m, 2H, CN–C_6H_4–O), 7.41 (m, 2H, (O)C–C_6H_4–O), 7.40 (d, J(H–H) = 5.5, 2H, $H_{\beta\text{-py}}$), 6.99 (m, 2H, CN–C_6H_4–O), 4.05 (t, J(H–H) = 6.5 Hz, –CH_2–O–C_6H_4), 1.83–1.27 (m, 16H, C_8H_{16}), 0.88 (t, J(H–H) = 6.6 Hz, 2H, CH_3). ^{19}F NMR (298 K, $CDCl_3$, coaxial tube of CF_3COOH in D_2O): −118.9 (m, 2F, F_o), −147.1 (m, 2F, F_m). FAB (+) m/z: 803.0 ($M + H^+$, calc.: 803.6). Anal. Calc. for $C_{35}H_{33}AuF_4N_2O_3$: C, 52.38; H, 4.14; N, 3.49. Found: C, 52.22; H, 4.11; N, 3.51%.

8b: Yield: 69%. IR (KBr, cm^{-1}): 2217 s, ν(C≡N), 1724 s, ν(C≡O), 1510 s, 1067 br, 956 s, 802 m,(C_6F_5). ^{1}H NMR (298 K, $CDCl_3$): 8.12 (d, J(H–H) = 8.7 Hz, 2H, (O)C–C_6H_4–O), 7.63 (d, J(H–H) = 8.8 Hz, 2H, CN–C_6H_4–O), 7.41 (d, J(H–H) = 8.7 Hz, 2H, (O)C–C_6H_4–O), 6.99 (d, J(H–H) = 8.8 Hz, 2H, CN–C_6H_4–O), 4.05 (t, J(H–H) = 6.5 Hz, –CH_2–O–C_6H_4), 1.83–1.28 (m, 16H, C_8H_{16}), 0.89 (t, J(H–H) = 6.6 Hz, 3H, CH_3). ^{19}F NMR (298 K, $CDCl_3$, coaxial tube of CF_3COOH in D_2O): −118.5 (m, 2F, F_o), −159.9 (t, $^3J_{F-F}$ = 20 Hz, 1F, F_p), −164.9 (m, 2F, F_m). FAB (+) m/z: 744.0 ($M + H^+$, calc.: 744.5). Anal. Calc. for $C_{30}H_{29}AuF_5NO_3$: C, 48,46; H, 3,93; N, 1,88. Found: C, 48.30; H, 4.01; N, 1.81%.

4. Crystal structure determination of complex 2b

4.1. Crystal data

$C_{31}H_{33}AuN_2O_3$, M = 678.56, triclinic, a = 6.574(5), b = 12.422 (7), c = 18.322(5) Å, α = 74.97(5), β = 85.91 (5), γ = 76.11(4)°, U = 1402.7(14) Å^3, space group $P\bar{1}$ (no. 2), Z = 2, λ = 0.71073 Å, μ(Mo Kα) = 5.277 mm^{-1}. The intensity data sets were collected at 150(2) K on a Bruker–Nonius KappaCCD diffractometer equipped

with an Oxford Cryostream 700 unit on a $0.60 \times 0.30 \times 0.10$ mm^3 prismatic colourless crystal. Multi-scan absorption correction was performed using the SORTAV program [24]. Although 16065 reflections were measured in a range from 3° to 27.5° in theta, the quality was quite poor, and two filters had to be applied to the data set to get a reasonable resolution, a limit of 20° in theta and $I > 2\sigma(I)$. The filtered set contained 3183 measured reflections, 1912 unique ($R_{int} = 0.147$) (73.5% completeness), which were used in all calculations. The structure was solved using the WINGX package [25], by direct methods (SHELXS-97) and refined by full-matrix least-squares against F^2 (SHELXL-97) [26] to give the final indices $R_1 = 0.118$ and $wR_2 = 0.294$, ratio data/parameters 1912/155. Final residues of 3.211 and –3.132 e Å^{-3} were located at 1.16 and 1.25 Å from Au1, respectively. Only the gold atom could be refined anisotropically and the hydrogen atoms were placed in calculated positions, refined using a riding model. Crystallographic data for the structural analysis has been deposited with the Cambridge Crystallographic Data Centre, CCDC No. 252120 for compound **2b**. Copies of this information may be obtained free of charge from: The Director, CCDC, 12 Union Road, Cambridge, CB2 1EZ UK. Fax. (int code) +44(1223)336 033 or Email: deposit@ccdc.cam.ac.uk or www.ccdc.cam.ac.uk.

Acknowledgements

Financial support for this work was provided by the DGICYT (Projects BQU2003-01131 and MAT2002-00562) and the CIRIT (Project 2001SRG00054). M.M. is indebted to the University of Barcelona for a scholarship.

References

[1] M. Ferrer, L. Rodríguez, O. Rossell, F. Pina, J.C. Lima, M. Font-Bardia, X. Solans, J. Organomet. Chem. 678 (2003) 82.
[2] M. Ferrer, M. Mounir, O. Rossell, E. Ruiz, M.A. Maestro, Inorg. Chem. 41 (2003) 5890.
[3] M. Ferrer, L. Rodríguez, O. Rossell, J. Organomet. Chem. 681 (2003) 158.
[4] (a) P. Espinet, Gold Bull. 32 (1999) 127;
(b) P. Alejos, S. Coco, P. Espinet, New J. Chem. 19 (1995) 799;
(c) S. Coco, P. Espinet, S. Falagán, J.M. Martín-Alvarez, New. J. Chem. 19 (1995) 959;
(d) M. Benouazzane, S. Coco, P. Espinet, J.M. Martín-Alvarez, J. Mater. Chem. (1995) 441.
[5] G. Jia, N.C. Payne, J.J. Vittal, R.J. Puddephatt, Organometallics 12 (1993) 4771.
[6] (a) R. Bayón, S. Coco, P. Espinet, C. Fernández-Mayordomo, J.M. Martín-Alvarez, Inorg. Chem. 36 (1997) 2329;
(b) S. Coco, C. Fernández-Mayordomo, S. Falagán, P. Espinet, Inorg. Chim. Acta 350 (2003) 366.
[7] A.C. Sarapu, R.F. Fenske, Inorg. Chem. 14 (1975) 247.
[8] M.J. Irwin, G. Jia, N.C. Payne, R. Puddephatt, Organometallics 15 (1996) 51.
[9] (a) See, for example: G. Jia, R.J. Puddephatt, J.J. Vittal, N.C. Payne, Organometallics 12 (1993) 263;
(b) Z. Assefa, B.G. McBurnett, R.J. Staples, J.P. Fackler, B. Assmann, K. Angermaier, H. Schmidbaur, Inorg. Chem. 34 (1995) 75;
(c) G.A. Carriedo, V. Riera, X. Solans, J. Solans, Acta Crystallogr. Sect. C 44 (1988) 978.
[10] T. Kaharu, R. Ishii, T. Adachi, T. Yoshida, S. Takahashi, J. Mater. Chem. 5 (1995) 687.
[11] D. Demus, L. Richter, in: Textures of Liquid Crystals, second ed., VEB, Leipzig, 1980.
[12] G.W. Gray, J.W. Goodby, in: Smectic Liquid Crystals. Textures and Structures, Hill, Glasgow, London, 1984.
[13] I. Dierking, in: Textures of Liquid Crystals, Wiley–VCH, Weinheim, 2003.
[14] K. Otha, H. Ema, Y. Morizumi, T. Watanabe, T. Fujimoto, I. Yamamoto, Liq. Cryst. 8 (1990) 311.
[15] T. Kaharu, R. Ishii, S. Takahashi, J. Chem. Soc., Chem. Commun. (1994) 1349.
[16] R.R. Lide (Ed.), Handbook of Chemistry and Physics, 73rd ed., CRC Press, Boca Raton, 1992.
[17] E.C. Constable, B. Karinki, A. Mahmood, Polyhedron 22 (2003) 687.
[18] M. Ferrer, M. Mounir, O. Rossell (in preparation).
[19] F. Neve, Adv. Mater. 8 (1996) 277.
[20] R. Usón, A. Laguna, Organomet. Synth. 3 (1986) 324.
[21] L.D. Ciana, A. Haim, J. Heterocycl. Chem. 21 (1984) 607.
[22] S. Takahashi, Y. Kuroyama, K. Sonogashira, N. Hagihara, Synthesis (1980) 627 (we have used $[Pd(PPh_3)_4]$ as a catalyst instead of $[PdCl_2(PPh_3)_2]$.).
[23] I.-Y. Wu, J.T. Lin, J. Luo, S.-S. Sun, C.-S. Li, K.-J. Lin, C. Tsai, C.-C. Hsu, J.-L. Lin, Organometallics 16 (1997) 2038.
[24] R.H. Blessing, Acta Crystallogr. Sect. A 51 (1995) 33.
[25] L.J. Farrugia, WINGX – A Windows Program for Crystal Structure Analysis, University of Glasgow, Glasgow, 1998.
[26] G.M. Sheldrick, SHELX97, Program for Crystal Structure Analysis (Release 97-2), Universität Göttingen, Germany, 1998.